*Biochimica et Biophysica Acta*, 1022 (1990) 57–71
Elsevier



BBAMEM 74705

# Transport parameters in the human red cell membrane: solute–membrane interactions of hydrophilic alcohols and their effect on permeation

Michael R. Toon and A.K. Solomon

*Biophysical Laboratory, Harvard Medical School, Boston, MA (U.S.A.)*

(Received 30 May 1989)

Key words: Erythrocyte membrane; Permeability; Water; Diol; Glycerol; Urea; Ethylene glycol; Reflection coefficient

**A systematic study has been made of the three coefficients that describe the human red cell membrane transport of a series of short straight-chain hydrophilic alcohols: the permeability coefficient, $\omega_i$, the reflection coefficient, $\sigma_i$, and the hydraulic conductivity, $L_p$. Ethylene glycol transport is saturable with $K_m = 220 \pm 50$ mM; there is a second, low-affinity, ethylene glycol site which inhibits water transport ($K_I = 570 \pm 140$ mM, max. inhib. = $90 \pm 10\%$). $\sigma_{eth\ gly} = 0.71 \pm 0.04$ which is significantly less than 1 ($n = 6$, $P < 0.001$), as are $\sigma_i$ for six other alcohols ($n = 23$), thus providing strong thermodynamic evidence that water and these alcohols cross the red cell membrane, at least in part, in an aqueous channel. The solute/membrane frictional coefficient, $f_{sm}$, for all seven alcohols has been determined and found to decrease monotonically as membrane permeability increases. The red cell membrane has been perturbed by treatments with phenylglyoxal and BS$^3$ (bis(succinimidyl suberate)); these treatments are accompanied by correlated modulation of both ethylene glycol and urea permeability. In one set of experiments in control cells, urea permeability is correlated with water permeability; and, in another set, ethylene glycol permeability is correlated with water permeability. All of these observations support the proposition that the urea class of solutes, the ethylene glycol class of solutes and water all cross the membrane through the same aqueous pore. A schematic model of the red cell pore, consistent with the experimental observations, is presented.**

## Introduction

In the course of our studies of the reflection coefficients, $\sigma_i$, of urea and ethylene glycol, we have developed a method to obtain values of the permeability coefficients, $\omega_i$, from the same data sets that were required to measure $\sigma_i$, making use of the simultaneous determination of the hydraulic conductivity, $L_p$, necessary for the determination of $\sigma_i$. We have applied these methods to a systematic study of the transport parameters of a series of short straight-chain hydrophilic alcohols.

Toon and Solomon [1] recently reported that high concentrations of urea inhibit water transport across the human red cell by binding to a site with $K_I = 550 \pm 80$ mosmolal. Other short chain hydrophilic amides and methyl-substituted ureas also inhibit hydraulic conductivity with well characterized $K_I$ values, so the urea site appears to be specialised for amide binding. We chose to characterize ethylene glycol and other alcohols in order to determine whether there is a similar low-affinity site for alcohol inhibition of water permeability and have found such a site with $K_I = 570 \pm 140$ mM and a maximum inhibition of $90 \pm 10\%$.

Separate simultaneous determinations of $\sigma_i$, $\omega_i$, and $L_p$ provide powerful insights into the impedances that govern membrane transport; we have been able to determine both $f_{sm}$, the solute/membrane friction and $f_{sw}$, the solute/water friction for each solute. We have found that $\sigma_i$ for each of seven alcohols is significantly different from 1 ($P < 0.01$–$0.025$) thus providing strong thermodynamic evidence that solute and water share a common pathway across part or all of the membrane. Finally we have found a number of correlations between water, urea and ethylene glycol transport, which provide further firm support for the view that these solutes and water cross the membrane through a common pore.

Supported in part by The Council for Tobacco Research - U.S.A., Inc., by the Squibb Institute for Medical Research and by the American Cancer Society, Massachusetts Division, Inc.

Correspondence: A.K. Solomon, Department of Physiology and Biophysics, Harvard Medical School, Boston, MA 02115, U.S.A.

## Materials and Methods

*Materials*

β-Mercaptoethanol and 1,2-propanediol were obtained from Eastman Organic Chemicals (Rochester, NY); butanediols (1,3-; 1,4-; 2,3-), 1,2,4-butanetriol, 1-(3,4-dichlorophenyl)-2-thiourea (DCPTU) and 2-(phenylthio)ethanol from Aldrich Chemical Co. (Milwaukee, WI); Hepes (*N*-2-hydroxyethylpiperazine-*N'*-2-ethanesulfonic acid) and Bis-Tris propane (1,3-bis[tris(hydroxymethyl)methylamino]propane) from Sigma (St. Louis, MO). Glycerol and ethylene glycol were supplied by Fisher Scientific (Fairlawn, NJ); $BS^3$, or BSSS, (bis(succinimidyl suberate)) by Pierce (Rockford, IL). All chemicals were of reagent grade. Outdated bank blood was kindly supplied by the Children's Hospital (Boston, MA).

*Methods*

Outdated bank blood, after aspiration of plasma and buffy coat, was washed three times with a buffer (stopped-flow buffer) of the following composition, in mM: NaCl, 142; KCl, 4.4; $MgCl_2$, 0.5; $CaCl_2$, 1.2; Hepes or Bis-Tris propane, 20 (pH 7.4; 300 ± 5 mosmolal). Osmolalities of all solutions were determined with a Fiske Model OS osmometer (Uxbridge, MA). Cells at 2% hematocrit were mixed with an equal volume of buffer made hyperosmolal by the addition of NaCl or permeant solute and the time course of red cell volume changes was measured using the stopped-flow apparatus of Terwilliger and Solomon [2]. Each numbered experiment was done with a different sample of blood. The analog data were digitized and averaged by a Hewlett-Packard Model 217 computer which was also used for the data analysis.

For the experiments with DCPTU, a stock solution of 25 mM DCPTU in ethanol was used to provide the inhibitor (maximum ethanol = 0.25% v/v) and an equivalent ethanol concentration was added to the control.

*Modification of cells with band 3 reagents*

Cells were modified with $BS^3$ according to Jennings et al. [3]. After three washes in 10 vol. of 150 mM KCl, 10 mM $Na_2HPO_4$ (pH 7.4) (PBK, 7.4 buffer) cells were resuspended at 50% hematocrit in the same medium containing freshly dissolved $BS^3$ (5 mM). After a 1-h incubation at 37° C, the reaction was stopped by adding 10 vol. of 50 mM glycine in PBK, 7.4. The cells were spun down and resuspended for 10 min at 20–23° C in PBK, 7.0 containing 0.2% bovine serum albumin (BSA). This was repeated once more, followed by two washes in our normal stopped-flow buffer as described above. Control experiments showed that treatment with $BS^3$ had no effect on the dependence of red cell volume on osmotic pressure.

Phenylglyoxal modification of cells was performed by a procedure adapted from Bjerrum et al. [4] as described by Jennings et al. [3]. Packed cells (in PBK, 7.4) were resuspended in 5 vol. of 0.1 M $Na_2HPO_4$ (pH 10.0) containing 10 mM phenylglyoxal for 5–15 min at 20–23° C. The cells were spun down and the reaction terminated by the addition of 10 vol. PBK, 6.0. The cells were then washed with PBK, 7.0 + 0.2% BSA as described above followed by washing in the stopped-flow buffer.

*Measurement of reflection coefficient*

The reflection coefficients, $\sigma_i$, reported in this paper were determined by the zero-time method of Goldstein and Solomon [5] as modified by Chasan and Solomon [6]. This method is based on the Kedem-Katchalsky equation for volume flow, $J_v$ ($cm^3 \cdot cm^{-2} \cdot s^{-1}$).

$$J_v = -L_p \Delta\pi_{imp} - \sigma_i L_p \Delta\pi_{perm} \quad (1)$$

in which the subscripts imp and perm represent impermeable and permeable solutes, $L_p$ is the hydraulic conductivity ($cm^3 \cdot dyn^{-1} \cdot s^{-1}$) and $\Delta\pi$ is the osmotic pressure difference across the membrane (osmol · $cm^{-3}$). One set of experiments is carried out in which $\Delta\pi_{imp}$ is varied, holding $\Delta\pi_{perm} = 0$, so that $L_p$ can be determined from the slope of $J_v$ against $\Delta\pi_{imp}$. A second analogous set of experiments is carried out to determine $\sigma_i L_p$ by varying $\Delta\pi_{perm}$, holding $\Delta\pi_{imp} = 0$. $\sigma_i$ is then determined directly from the ratio of the slopes.

$\Delta\pi_{perm}$ is known accurately at zero time, but once the cells have been mixed with hyperosmolal buffer in the stopped-flow apparatus, both water and solute move across the membrane and $\Delta\pi_{perm}$ can no longer be determined from measurements of the time course of cell volume change. Consequently $J_v$ is extrapolated to its zero-time value and the initial values of both $\Delta\pi$ gradients are used for the computation. For each mixing solution, twenty-five consecutive runs were averaged. Data were usually collected over the range of 4–8 ms to 1 s and the averaged cell volume/time records were corrected for light-scattering intensity changes not associated with volume changes by subtraction of the same number of control runs in which the blood suspensions were mixed with isosmolal buffer solutions (± permeant solutes) as described by Levin et al. [7].

Toon and Solomon [8] developed a curve-fitting method for determining $J_{v,t=0}$ accurately, with minimal curve-fitting bias. Each difference curve was fitted to a second degree polynomial ($a_1 + a_2 t + a_3 t^2$) by non-linear least squares from 8.5 ms to 260 ms. The slope of the curve at zero time (approx. 8.5 ms) is given directly by the coefficient for the first-order term of the polynomial (neglecting a small contribution of approx. 2–4% for $2a_3 t$ at 8 ms). A range of 4–5 initial NaCl gradients of 150 to 400 mosmolal (after mixing) was used to

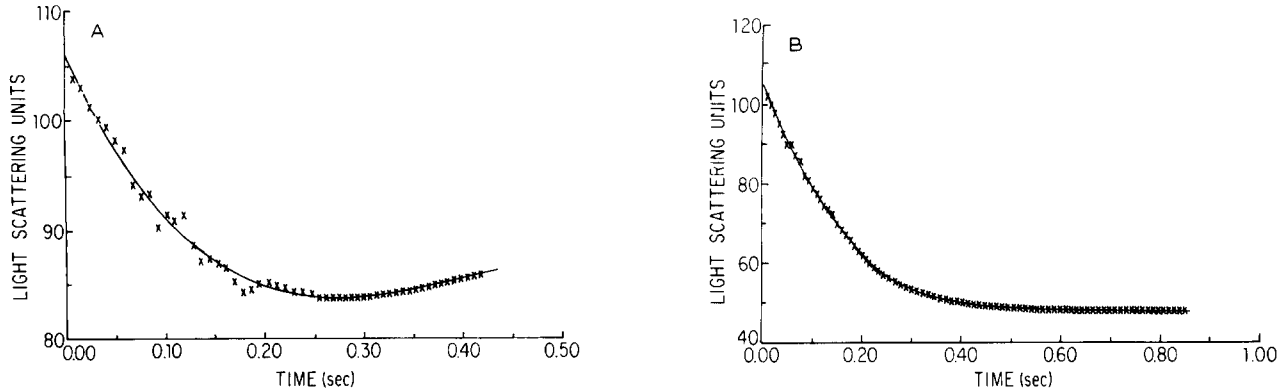


Fig. 1. (A) Non-linear least-squares fit of typical experimental data for $\omega_{\text{eth gly}}$ to a third order polynomial, as described below Eqn. 2 (B) Non-linear least-squares fit of experimental data for $L_p$ to the $L_p$ equation in footnote on p. 60.

determine the hydraulic conductivity from the slope of the initial rate of volume change, measured in light-scattering units (lsu), versus the osmotic pressure difference, as discussed in our previous paper [8]. Since we only report ratios of permeability coefficients in these experiments (fractional inhibition of hydraulic conductivity or determination of the reflection coefficient), light-scattering units do not have to be converted to cell volume units, so long as the conversion ratio remains constant [1]. We have terminated the fitting procedure at about the minimum volume for each permeant solute in order not to compromise the initial course of the polynomial by events which are dominated by the solute permeation.

*Solute inhibition experiments*

Eqn. 1 can not be used to determine $L_p$ in the presence of a permeant solute concentration gradient for the same reason that it cannot be used to determine $\sigma_i$. However, if the permeant solute is at the same concentration on both sides of the membrane at zero-time, $\Delta\pi_{\text{perm}, t=0}$ is zero and the effect of a permeant solute on $L_p$ can be measured from zero-time slopes, just as in the determination of $\sigma_i$. Consequently, the permeant solutes were added at the same concentration, both to the red cell suspensions and to the solution with which the cells were to be mixed, so that, at zero time, the only gradient present was that imposed by the NaCl, which makes it possible to determine how $L_p$ is modulated by addition of a permeant solute. As above, cells at 2% hematocrit in isosmotic buffer were mixed with an equal volume of buffer made hyperosmolal by the addition of either NaCl or permeant solute, and for each mixing solution, twenty-five consecutive runs were averaged and corrected by the subtraction of control runs. In these experiments, we have reported the concentration dependence of the permeant solute inhibition, so it has been necessary to translate the data from light-scattering units (lsu) to absolute volume units, though this means that we have implicitly assumed that lsu are linearly dependent on cell volume, over the concentration range we have used, as previously discussed (Toon and Solomon [1]).

*Measurement of permeability coefficient*

The permeability coefficients, $\omega_i$, were determined by the minimum method of Sha'afi et al. [9]. In these experiments, cells in isosmotic buffer are mixed with the same buffer to which a permeant solute, alone, is added. Under these conditions the cells first shrink to a minimum volume and then swell again to their final volume when both the activity gradients of the permeant solute and of the water have fallen to zero. $\omega_i$ is determined from the second derivative of the rate of volume change at the minimum volume, $(d^2V'/dt^2)_{\text{min}}$, together with the ratio of the minimum volume to the original volume, according to the equations given in Sha'afi et al. [9]:

$$\omega_i = V'_{\text{min}}(d^2V'/dt^2)_{\text{min}}/A^2L_pRT\left(\pi^{\text{o}}_{\text{imp}} - \pi^{\Delta x}_{\text{imp}}\right) \quad (2)$$

in which $V'$ is the volume of cell water and $\pi_{\text{imp}}$ is the osmotic pressure of the impermeant solute at the outside of the cell (superscript, o) or inside ($\Delta x$). $A$ is the red cell area, taken as $1.35 \cdot 10^{-6}$ cm$^2$, following Jay [10], and $R$ and $T$ have their usual meanings. The data are fitted by non-linear least squares to a third-order polynomial over the range from zero time to just past the minimum volume and $d^2V'/dt^2$ is obtained from the slope at the minimum volume; a typical polynomial fit to the data from twenty-five averaged runs is shown in Fig. 1 (left). Computation of $\omega_i$ also requires knowledge of the fractional cell water content, 0.71 under isosmolal conditions (Savitz et al. [11]), and the fraction of non-osmotic water, taken as 0.43 (see Solomon et al. [12]).

For each measurement of $\omega_i$, $L_p$ was determined at the same time with cells under identical conditions, in cell volume units rather than light-scattering units, using the entire time course (rather than the initial slope) of

TABLE I

*Reflection coefficient for alkanols*

The number of experiments (each on a different blood) is given in parentheses (errors are S.D. of the mean). $P$ is the probability that $f(\sigma_i) = 0$, determined by the $t$ test.

| | $\bar{V}$ ($cm^3 \cdot mol^{-1}$) | $(\omega\bar{V}/L_p)$ | $\sigma$ | $f(\sigma_i)$ | $P$ |
|---|---|---|---|---|---|
| Ethylene glycol | 56.0 | 0.033 | $0.71 \pm 0.04$ (6) | $0.26 \pm 0.02$ | 0.001 |
| 1,2-Propanediol | 71.8 | 0.016 | $0.75 \pm 0.04$ (4) | $0.23 \pm 0.01$ | 0.001 |
| 1,4-Butanediol | 88.6 | 0.020 | $0.68 \pm 0.07$ (5) | $0.30 \pm 0.03$ | 0.001 |
| 1,3-Butanediol | 89.6 | 0.024 | $0.68 \pm 0.06$ (3) | $0.30 \pm 0.03$ | 0.0025 |
| 2,3-Butanediol | 91.3 | 0.050 | $0.56 \pm 0.08$ (5) | $0.39 \pm 0.06$ | 0.001 |
| 1,2,4-Butanetriol | 104.2 | 0.007 | $0.84 \pm 0.05$ (3) | $0.15 \pm 0.01$ | 0.0025 |
| Glycerol | 73.0 | 0.007 | $0.88 \pm 0.03$ (3) | $0.11 \pm 0.01$ | 0.001 |

volume change to fit the equation for $L_p$ given * by Levin et al. [7]. As above, the averaged cell volume/time records were corrected by subtraction of control runs prior to further analysis. The averaged data from a series of twenty-five consecutive runs was fit by a non-linear least-squares program written by Dix (private communication); a typical fit is shown in Fig. 1 (right). The $L_p$ program provided the conversion data needed to express $\omega_i$ in units of cell volume (rather than light-scattering units).

## Results

*Determination of $\sigma_i$ and $\omega_i$ for hydrophilic straight chain alcohols*

There are two major molecular determinants that govern the passage of small hydrophilic molecules across the red cell membrane: the size of the molecule, and its ability to form hydrogen bonds; and there are two thermodynamic parameters that describe the interaction of the $i$th solute with the membrane: $\sigma_i$ and $\omega_i$. We have made a systematic study of the relation between the molecular determinants and the phenomenological parameters for a series of straight-chain hydrophilic alcohols. The number of solutes is limited by practical considerations since they must be small enough to go through the pore, and hydrophilic enough that lipid permeability may be neglected. We had initially intended only to measure the reflection coefficients because the permeability coefficients of a number of these alcohols had previously been measured by Sha'afi et al. [14]. However, in the course of our studies, we developed the computational techniques to extract the permeability coefficients from the same data set which had already been used for the $\sigma_i$ measurements and so we have also determined the $\omega_i$.

A thermodynamic answer to the question of whether permeating solutes enter the cell through an aqueous channel can be obtained from $\sigma_i$ determinations. If the inequality, $\sigma_i < [1 - (\omega_i \bar{V}_i / L_p)]$, is satisfied ($\bar{V}_i$ is the partial molar volume of $i$), it provides the strongest thermodynamic evidence that water and the solute interact in an aqueous pore over a significant fraction of their passage across the membrane ** (Katchalsky and Curran [17]). The largest number of measurements of $\sigma_i$ and the inequality was made for ethylene glycol which served as a common reference point for all of our $\sigma_i$ determinations in the alcohol series. Table I shows the average value of $\sigma_{\text{eth gly}}$ to be $0.71 \pm 0.04$, which is the same as the previous value of $0.71 \pm 0.03$ given by Toon and Solomon [8]. In all we have carried out 15 de-

* The equation given by Levin et al. (Ref. 7, their equation 3) contains some misprints. The equation, as corrected by Solomon [13], is:

$$L_p = \frac{V_{c,iso}}{ART(\pi^o)^2 t} \pi^i_{iso} [1 - (V_b / V_{c,iso})] \times \left( \ln \frac{\pi^i_{iso} - \pi^o}{\pi^i_{iso} - Q\pi^o} - \frac{\pi^o [(V_c / V_{c,iso}) - 1]}{\pi^i_{iso} [1 - (V_b / V_{c,iso})]} \right)$$

In this notation, the superscript, i, refers to the inside of the cell. The subscript, iso, refers to isosmolar conditions. $V_b$ is the apparent non-osmotic water plus cell solutes and membrane volume, as determined from a plot of cell volume, $V_c$, as function of medium osmolality, which follows the following equation:

$$\hat{V}_c = (1 - \hat{V}_b) \pi^i_{iso} / \pi^i + \hat{V}_b$$

Volumes have been normalized so that $\hat{V}_c = V_c / V_{c,iso}$ and $\hat{V}_b = V_b / V_{c,iso}$.

$$Q = [(\hat{V}_c - \hat{V}_b)/(1 - \hat{V}_b)]$$

** The term, $\omega_i \bar{V}_i / L_p$, arises from the contribution of solute permeability by dissolution in the membrane to the computation of $\sigma_i$. This point is discussed by Kedem and Katchalsky (Ref. 15, Eqn. 64) and explained clearly by Dainty (Ref. 16, Eqns. 57–59). Table I shows that $\omega_i \bar{V}_i / L_p$ is small both compared to $\sigma_i$ and to 1.0. Therefore, the values for $f_{sm}$ and $f_{sw}$ refer to frictional coefficients in the aqueous channel and not to any frictional terms resulting from solute passage through the membrane fabric by dissolution.

terminations of $\sigma_{\text{eth gly}}$ and the agreement among our values means that there is essentially no statistical possibility that our value could agree with that of 1.0, given by Levitt and Mlekoday [18].

The values of $\sigma_i$ that we have obtained for the other alcohols are also given in Table I, and it is apparent that all of these values are $< 1.0$. Table I also gives the numerical value of the inequality, expressed as

$$f(\sigma_i) = 1 - (\omega_i \bar{V}_i / L_p) - \sigma_i \qquad (3)$$

The last column gives the probability that $f(\sigma_i)$ is significantly different from zero. In five cases, the probability that the inequality is zero is 0.1% ($t$ test) and in the other two cases, the probability is 0.25%. Thus, the probability that $\sigma_i$ actually equals $(1 - (\omega_i \bar{V}_i / L_p))$ in these 29 measurements is vanishingly small and we may safely conclude that water and the hydrophilic alcohols that we have studied interact in an aqueous pore as they traverse the membrane.

Since our determination of $\omega_i$ is a byproduct of our $\sigma_i$ determinations, we have obtained data for $\omega_i$ at all the solute concentrations required for the $\sigma_i$ determinations. Fig. 2 shows the average ethylene glycol influx in five experiments, as a function of solute concentration over the range from 0.2 to 0.6 M. The flux is saturable with $K_m = 220 \pm 50$ mM, in good agreement with the results of Mayrand and Levitt [19], who had previously reported that ethylene glycol flux was saturable with $K_m = 175 \pm 22$ mM. None of the other alcohols, whose permeability coefficients were determined over the same concentration range, showed any evidence of a saturable site. $\omega_{\text{eth gly}}$ varies from $(12.2 \pm 1.8) \cdot 10^{-15}$ mol · dyn$^{-1}$ · s$^{-1}$ at 0.2 M to $(6.5 \pm 1.6) \cdot 10^{-15}$ mol · dyn$^{-1}$ · s$^{-1}$ at 0.6 M. In Table II, which contains the values for $\omega_i$ for the alcohols (column 2), we have used the value at 0.4 M, the midpoint in the range, as the value for

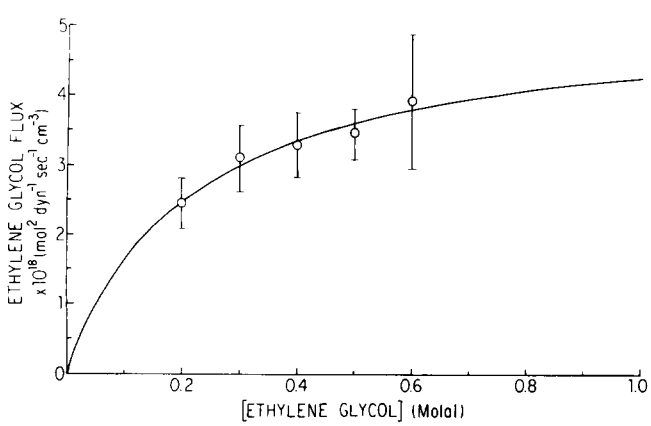


Fig. 2. Concentration dependence of ethylene glycol flux. $\omega_{\text{eth gly}}$ has been multiplied by the [ethylene glycol] (M) at which it was determined to obtain the flux. Average of five determinations showing S.D. of the mean; fitted to a single-site binding curve by non-linear least squares. $K_m = 220 \pm 50$ mM.

TABLE II

*Permeability and frictional coefficients for alkanols*

| | Permeability coefficient, $\omega_i$ ($10^{-15}$ mol · dyn$^{-1}$ · s$^{-1}$) | Frictional coefficients ($10^{16}$ dyn · s · mol$^{-1}$ · cm$^{-1}$) | |
|---|---|---|---|
| | | $f_{sw}$ | $f_{sm}$ |
| Red blood cell | | | |
| Ethylene glycol | 8.3 ± 1.2 * | 9.91 | 26.2 |
| 1,2-Propanediol | 2.9 ± 0.1 | 25.2 | 84.4 |
| 1,4-Butanediol | 2.2 ± 0.1 | 43.4 | 101 |
| 1,3-Butanediol | 4.4 ± 0.1 | 21.7 | 50.6 |
| 2,3-Butanediol | 7.1 ± 0.2 | 17.5 | 27.4 |
| 1,2,4-Butanetriol | 1.1 ± 0.1 | 43.4 | 246 |
| Glycerol | 1.4 ± 0.1 | 25.0 | 202 |
| Dialysis tubing (Ginzburg and Katchalsky [23] | | | |
| Glucose | | 1.79 | 0.31 |
| Sucrose | | 3.12 | 0.73 |

[a] Computed from fitted curve in Fig. 2 for 0.4 M ethylene glycol.

$\omega_{\text{eth gly}}$, which should be comparable with the other alcohols whose permeability coefficients are given in Table II.

The permeability coefficients for three and four-carbon alcohols in Table II are larger than those determined in this laboratory in 1971 by Sha'afi et al. [14]. One reason for the discrepancy is the difference in the red cell surface area which has subsequently been measured more accurately (present value, $1.35 \cdot 10^{-6}$ cm$^2$ (see Jay, Ref. 10); previous value, $1.67 \cdot 10^{-6}$ cm$^2$). Since the area enters as the square in the denominator of Eqn. 2 for $\omega_i$, this effect leads to a correction, increasing the values given by Sha'afi et al. [14] by a factor of 1.6. With this correction, the present values are about 50% higher than the previous ones *; the ratio

* The actual parameter determined in the estimation of $\omega_i$ is $\omega_i L_p$ from which $\omega_i$ is obtained by division by $L_p$ (in the denominator of the right hand side of Eqn. 2). Therefore, attention must be paid to the effect of differences in $L_p$ caused by differences in the $V/A$ ratio used in the measurements of Sha'afi et al. [14] and our own. The present value of $V/A$ is $7.41 \cdot 10^{-5}$ cm; the value used by Rich et al. [20] was $5.21 \cdot 10^{-5}$ cm, and Sha'afi et al. [14] used the $L_p$ value of Rich et al. for their determination of $\omega_i$. The matter is complicated even more by changes in the characteristic value of $L_p$ which we have tentatively attributed to the fact that we now routinely use bank blood, while Rich et al. [20] used fresh blood and found that $L_p = 1.3 \cdot 10^{-11}$ cm$^3$ · dyn$^{-1}$ · s$^{-1}$ which, after correction to the present $V/A$, would become $1.8 \cdot 10^{-11}$ cm$^3$ · dyn$^{-1}$ · s$^{-1}$, in good agreement with the value of $1.8 \cdot 10^{-11}$ cm$^3$ · dyn$^{-1}$ · s$^{-1}$ determined by Terwilliger and Solomon [2] for fresh blood. Our present typical values for bank blood are $L_p = 1.4 \cdot 10^{-11}$ cm$^3$ · dyn$^{-1}$ · s$^{-1}$. Under the circumstances, we do not feel it is warranted to make any corrections for the differences in $L_p$. In the present experiments, we have used individual values of $L_p$, determined on the same blood, and at the same time, in our use of Eqn. 2 to obtain the values for $\omega_i$ given in Table II.

among the permeabilities of the alcohols, one to another, is closely similar in the two studies.

In the case of ethylene glycol, whose permeability was measured by Savitz and Solomon in 1971 [21], the agreement is better. Their figure, which needs to be increased by only the first power of the ratio of the areas since it was obtained by tracer diffusion, comes to $(8 \pm 1) \cdot 10^{-15}$ mol · dyn$^{-1}$ · s$^{-1}$, after correction, in good agreement with the present computed figure of $(8.3 \pm 1.2) \cdot 10^{-15}$ mol · dyn$^{-1}$ · s$^{-1}$. Mayrand and Levitt's value is $19.6 \cdot 10^{-15}$ mol · dyn$^{-1}$ · s$^{-1}$ ('in the low concentration limit'), higher than our highest value of $(12.2 \pm 1.8) \cdot 10^{-15}$ mol · dyn$^{-1}$ · s$^{-1}$ at 0.2 M ethylene glycol by a factor of 1.5, which may reflect a difference in ethylene glycol concentration.

*Determination of solute-membrane and solute-solvent frictional coefficients*

The frictional treatment of passage through aqueous channels given by Katchalsky and Curran [17], predicts that $f(\sigma_i)$ should depend upon $\omega_i$ according to the following equation:

$$f(\sigma_i) = 1 - (\omega_i \bar{V}_i / L_p) - \sigma_i = \omega_i (f_{sw} \Delta x / \varphi_w) \quad (4)$$

in which $\Delta x$ is the membrane thickness, taken as 40 Å and $\varphi_w$ is the fractional water content of the membrane which can be estimated as 0.13%, as calculated * by Solomon et al. [22] from the restriction of free diffusion of water across the red cell. $f_{sw}$ has been defined by Katchalsky and Curran [17] as 'the frictional coefficient between a mole of solute and an infinite amount of water' and its use is illustrated by their observation that, in the limit of diffusion through very large pores, $f_{sw}$ approaches the value for free solution, $f_{sw}^0$. $f_{sw}^0$ is equal to $RT/D_i$, in which $D_i$ is the diffusion coefficient and $RT$ has its usual meaning. Rearranging Eqn. 4 shows that

$$f_{sw} = f(\sigma_i) \varphi_w / \omega_i \Delta x \quad (5)$$

Two other frictional coefficients, $f_{sm}$ and $f_{wm}$, are required to transform the equations for membrane transport from phenomenological to frictional terms (Katchalsky and Curran [17]). $f_{wm}$ is the coefficient of friction between water and the membrane, whose relation to $L_p$ (in the absence of an osmotic pressure gradient) is given by:

$$f_{wm} = \varphi_w \bar{V}_w / L_p \Delta x \quad (6)$$

similar to the relationship between $f_{sw}$ and $D$. $f_{sm}$ is the frictional coefficient between the solute and the membrane, which has been expressed in terms of its phenomenological equivalents by Ginzburg and Katchalsky [23], who give:

$$f_{sm} = f_{sw} [(1 - f(\sigma_i)) / f(\sigma_i)] \quad (7)$$

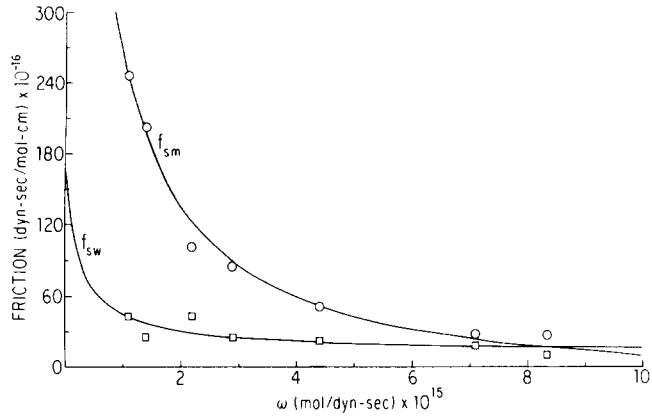


Fig. 3. Dependence of frictional coefficients, $f_{sm}$ and $f_{sw}$ on $\omega_i$. The data have been fitted by non-linear least squares to an empirical equation of the form: $f_{(sm\ or\ sw)} = A(3) + (A(2)\omega_i / [A(1) + \omega_i])$. For $f_{sw}$, $A(1) = 0.25 \pm 0.19$; $A(2) = -161 \pm 87$; $A(3) = 173 \pm 88$. For $f_{sm}$, $A(1) = 0.29 \pm 0.04$; $A(2) = -1280 \pm 117$; $A(3) = 1255 \pm 118$. The units of $A(1)$ are $10^{-15}$ mol · dyn$^{-1}$ · s$^{-1}$; those of $A(2)$ and $A(3)$ are $10^{16}$ dyn · s · mol$^{-1}$ · cm$^{-1}$.

The frictional coefficients computed from Eqns. 5 and 7 are given in Table II, which also contains data on the frictional coefficients for glucose and sucrose passage across dialysis tubing, as measured by Ginzburg and Katchalsky [23]. The frictional coefficients for dialysis tubing are very much smaller than those we have obtained for red cell permeation, consistent with the 23 Å pore radius for dialysis tubing (Ginzburg and Katchalsky [23]) very much larger than the $6.5 \pm 0.6$ Å equivalent pore radius for the red cell (Solomon [24]).

Fig. 3 provides a graphical illustration of the relative importance of solute-membrane and solute-solvent frictions as determinants of solute permeability. $f_{sm}$ is the dominant factor for the larger and least permeable solutes, which are almost as large as the pore; Sha'afi et al. [14] give 2.6–3 Å for the cylindrical radius of the butanediols, determined from molecular models. These are unhydrated radii and the addition of the hydration shell, which would add a significant fraction of the 3.0 Å required for a complete single shell, means that collisions with the pore wall, with its 6.5 Å radius, would dominate. Examination of Table II shows that $f_{sm}$ is always greater than $f_{sw}$, usually by a factor of two or more, for all the alkanols whose permeability we

* Solomon et al. [22] computed that there were $2.7 \cdot 10^5$ pores in the red cell membrane, based on a construct with a diffusion hindrance factor of 0.064, an equivalent pore radius of 4.5 Å, $D_{water} = 2.3 \cdot 10^{-5}$ cm$^2$ · s$^{-1}$ and a red cell area of $1.35 \cdot 10^{-6}$ cm$^2$. Assuming these to be uniform right cylindrical pores leads to the figure of 0.13% for the water content of the membrane, $\varphi_w$. Since $\varphi_w$ only appears in Eqn. 5 as a scale factor, effectively as part of the ratio, $\varphi_w / \omega_i$, the assumptions involved in the evaluation of $\varphi_w$ do not affect the relation among the frictions of the various solutes or between $f_{sw}$ and $f_{sm}$.

have measured. It is only when the pore radius is very large compared to the solute radius that solute-solvent friction dominates the process, as shown by the data of Ginzburg and Katchalsky [23] for diffusion of the small glucose molecule (unhydrated radius ≈ 3.6 Å, see Ref. 24), through the 23 Å radius pores in dialysis tubing. In this case, $f_{sw}$ becomes four to 5-times larger than $f_{sm}$ in these very large channels, as Table II shows. The coherent picture of hydrophilic solute passage across the red cell membrane provided by these frictional coefficients and the relationships among them illustrated in Fig. 3 provide further strong support for the conclusion that small hydrophilic straight-chain alcohols cross the red cell membrane through an aqueous channel.

Comparison among the various alcohols illustrates the effect of addition of a single -OH group on $f_{sm}$. The three narrow black arrows in Fig. 4 show that addition of a single -OH group increases $f_{sm}$ by as much as a factor of eight when the addition is made to a terminal methyl, and a smaller factor, when the addition is made to an internal methylene group. Since the addition of an -OH group has a very large effect on H-bonding and a relatively small effect on molecular size, these comparisons show that H-bonding with the channel walls is an

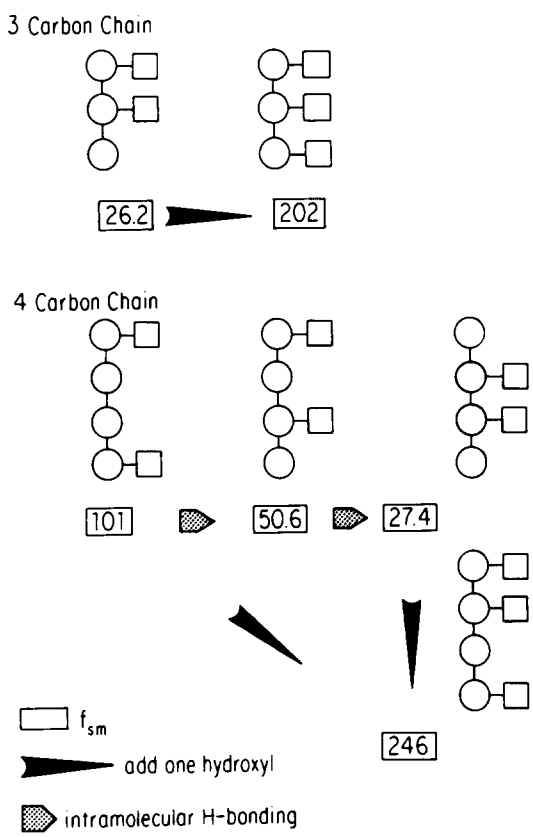


Fig. 4. Effects of hydroxyl groups and intramolecular H-bonds on $f_{sm}$. Data for $f_{sm}$ from Table II are shown in square boxes. Solid arrows show progression by addition of a single hydroxyl group and stippled arrows show the effects produced by apposition of hydroxyl groups in butanediol.

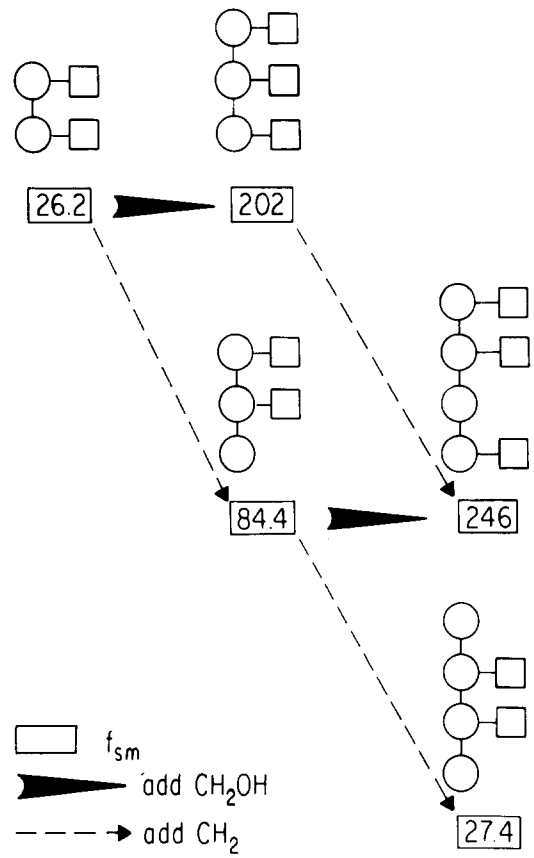


Fig. 5. Effects of addition of $CH_2$ (dashed arrows) and $CH_2OH$ groups (filled arrows) on $f_{sm}$ using data from Table II (in boxes).

important determinant of membrane permeability. The effect of intramolecular hydrogen bonding is shown by the horizontal procession along the broad stippled arrows in the central row. As the -OH groups move close together, intramolecular H-bonding is significantly strengthened and the friction with the membrane correspondingly decreased, providing a further illustration of the importance of membrane hydrogen bonding to solute permeation.

Addition of a $-CH_2OH$ group is straightforward since it increases both steric hindrance and hydrogen bonding, producing a consistent increase in $f_{sm}$ as evidenced by the horizontal black arrows in Fig. 5. The steric effects can be singled out by examining the effect of addition of $-CH_2$ groups which increase the size of the molecule with no direct effect on H-bonding. Advancement along the dashed diagonal lines in Fig. 5 shows that both the change from ethylene glycol to 1,2-propanediol and that from glycerol to 1,2,4-butanetriol cause a large increase in $f_{sm}$. These results provide a further instance of the importance of H-bonds and show also that steric hindrance impedes membrane permeation.

The transition between 1,2-propanediol and 2,3-butanediol is anomalous because the addition of a $-CH_2$ group decreases $f_{sm}$ from $84.4 \cdot 10^{16}$ dyn · s · mol$^{-1}$ ·

$cm^{-1}$ to $27.4 \cdot 10^{16}$ $dyn \cdot s \cdot mol^{-1} \cdot cm^{-1}$, rather than increasing $f_{sm}$ as expected. 2,3-Butanediol is anomalous in another respect, as shown by the unusually high value for $(\omega \bar{V}/L_p)$ in Table I (column 3). As Dainty (16) points out, $(\omega \bar{V}/L_p)$ is the correction term for passage through the membrane fabric, so that $f_{sm}$ applies only to friction within the aqueous channel. The observation that $(\omega \bar{V}/L_p) = 0.05$, virtually twice as great as any other alcohol means that the membrane solubility of 2,3-butanediol is very much greater than any of the other polyhydric alcohols we have studied. This conclusion is supported by the measurement of Collander [25] of the ether/water partition coefficient, which is 0.029 for 2,3-butanediol, 50% higher than the figure of 0.018 for 1,2-propanediol. These observations mean that the intramolecular H-bonding capacity of 2,3-butanediol is appreciably more than that of 1,2-propanediol, consistent with the reduction of $f_{sm}$.

*Inhibition of water permeability by ethylene glycol*

When Toon and Solomon [1] reported that urea concentrations in the 0.3–1 M range caused red cell water permeability to decrease by up to 80%, they pointed out that this decreased permeability would protect the red cells against excessive dehydration as the cells passed through the high urea environment in the kidney inner medulla. Although there is no physiological reason to expect a similar inhibition by ethylene glycol, we carried out an analogous set of experiments with ethylene glycol and obtained an analogous result, as shown in Fig. 6. In five experiments, $K_{I,\,eth\,gly} = 570 \pm 140$ mM, with a maximum inhibition of $0.9 \pm 0.1$, identical with the values for urea ($K_{I,\,urea} = 550 \pm 80$ mM, maximum inhibition $= 0.82 \pm 0.06$). We have underlined the similarity between the two inhibitors by showing the fitted curve for urea inhibition (from Ref. 1) as the dashed line in Fig. 6.

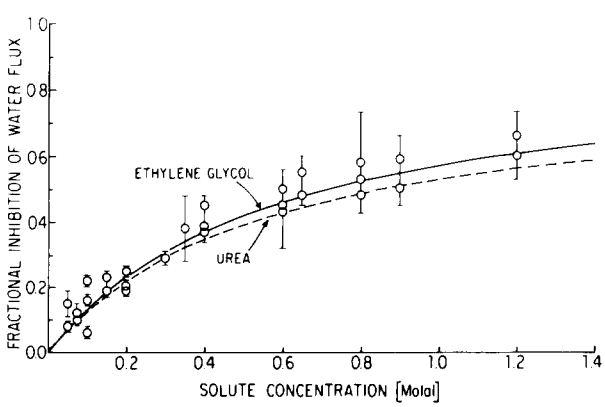


Fig. 6. Fractional inhibition of osmotic water flux by ethylene glycol. Data from five experiments (means ± S.E.). Data have been fitted by non-linear least squares to a single site binding curve (full line) with $K_I = 570 \pm 140$ mM (max. inhib. $= 0.9 \pm 0.1$). The dashed curve for urea inhibition is taken from Ref. 1 ($K_I = 550 \pm 80$ mM; max. inhib. $= 0.82 \pm 0.06$).

At first sight, the similarity between these $K_I$ values suggests that the inhibition site exhibits no molecular specificity at all, but this is clearly not the case. Toon and Solomon [1] showed that the short-chain aliphatic amides which inhibit urea permeation also inhibit water permeation; creatinine, which is a heterocyclic amine, with no effect on urea permeation, also has no effect on water flux. Furthermore, Toon and Solomon [1] pointed out that there is a relationship between the $K_I$ values for amide inhibition of urea flux and those for amide inhibition of water flux. The data suggest a linear correlation (correlation coefficient, 0.87; slope $(K_{I,\,urea\,inhib}/K_{I,\,water\,inhib}) = 3.5 \pm 1.1$). If the same site mediated both urea and water transport, the slope should be unity; it is hard to understand how the binding for water inhibition can be so much less tight than that for urea inhibition. The present finding that ethylene glycol also inhibits water transport adds an additional piece of evidence that will have to be incorporated in any coherent explanation of the mechanism of the water transport inhibition process.

*The familial relationship of alcohol and amide classes of transport sites and the use of thiol analogs to characterize them*

Thio-substituted urea derivatives have been used widely to study urea transport ever since Wieth et al. [26] showed that thiourea was a potent inhibitor of urea permeability. In general urea transport inhibitors are primarily effective on amide transport, with little or no effect on alkanols. Thus, Solomon and Chasan [27] showed that thiourea also inhibits formamide and acetamide transport, but has no effect on glycerol or longer chain, lipid-soluble amides. Mayrand and Levitt [19] reported that formamide and acetamide inhibit urea transport, with $K_I = 100$ mM. They also found that thionicotinamide, which inhibits urea transport with $K_I = 0.1$ mM, has no effect on ethylene glycol permeability at 1 mM, though glycerol inhibits ethylene glycol permeability with $K_I = 1200$ mM. All these observations are consistent with separate H-bonding regions for transport of amides and alcohols.

We have previously suggested [22] that the efficacy of thiourea as an inhibitor of urea transport might be related to the proximity of the H-bonding site to membrane lipids, because thiol substitution increases lipid solubility. Since it is also likely that the H-bonding site for ethylene glycol is adjacent to the membrane lipids, we decided to investigate the effect of thiol substitution on ethylene glycol and glycerol transport. In a set of preliminary experiments, Balkanski (private communication) found that β-mercaptoethanol, the thiol analog of ethylene glycol, did not affect urea permeation, though it did inhibit both ethylene glycol and glycerol permeation, as we subsequently confirmed. The results in Fig. 7 show that both ethylene glycol and glycerol

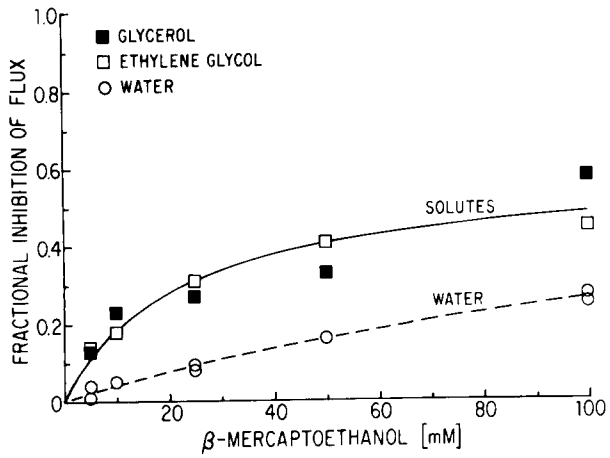


Fig. 7. β-Mercaptoethanol inhibition of water and alcohol fluxes. The data for inhibition of glycerol and ethylene glycol fluxes are from one experiment, typical of two. The data were fitted by non-linear least squares to a single site binding curve with $K_I = 22 \pm 7$ mM (max. inhib. $= 0.59 \pm 0.07$). The data for inhibition of water flux are from two experiments and have been fitted to a single site binding curve with $K_I = 160 \pm 40$ mM (max. inhib. $= 0.7 \pm 0.1$).

permeability are inhibited with the same $K_I$ of $22 \pm 7$ mM (maximum inhibition $0.59 \pm 0.07$), very much smaller than the $K_m$ of $220 \pm 50$ mM for self-saturation of ethylene glycol permeability. Thus, thiol substitution also increases the binding affinity of the alcohols. Mayrand and Levitt [19], in an extensive series of experiments, had shown that aromatic substitution in thiourea compounds increased the inhibition binding affinity by more than an order of magnitude, the inhibition constant for phenylthiourea being 0.4 mM, as compared to 19 mM for thiourea. We studied the effect of aromatic substitution with 2-(phenylthio)ethanol at concentrations of 1–2 mM and found an average inhibition of ethylene glycol flux of 0.80 (0.84 and 0.75, two experiments) which provides further evidence both of the importance of lipid solubility and the analogy between the urea/amide and the alcohol families.

β-Mercaptoethanol also inhibits water transport with $K_I = 160 \pm 40$ mM, as can be seen in the bottom curve in Fig. 7. This $K_I$ is very much smaller than the $K_I$ of 570 mM for ethylene glycol inhibition of water flux, consistent with a water transport inhibition site adjacent to a lipid environment. Comparison of the two fitted curves in Fig. 7 shows clearly than the β-mercaptoethanol low-affinity site for water transport inhibition differs substantially from the higher-affinity site for inhibition of ethylene glycol and glycerol transport, analogous to the observations in the urea/amide family.

*Model of red cell water transport channel*

Our model of the red cell water channel is an

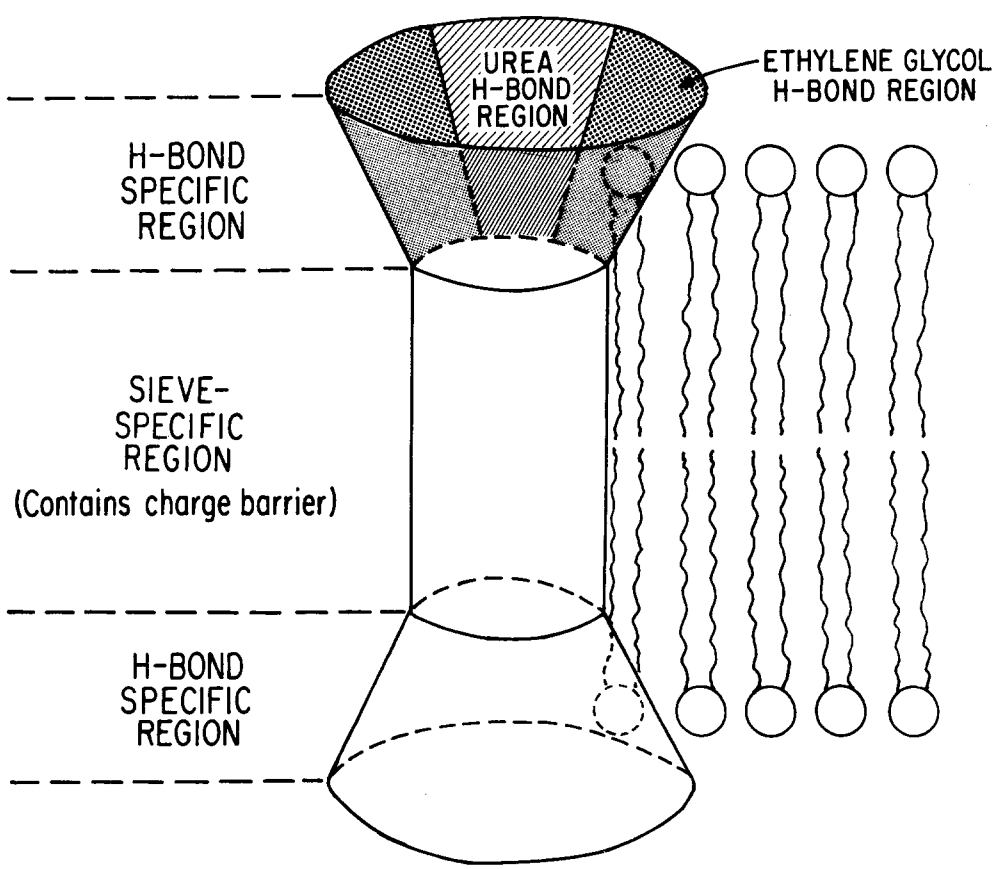


Fig. 8. Schematic drawing of red cell pore showing separate H-bond-specific and sieve-specific regions.

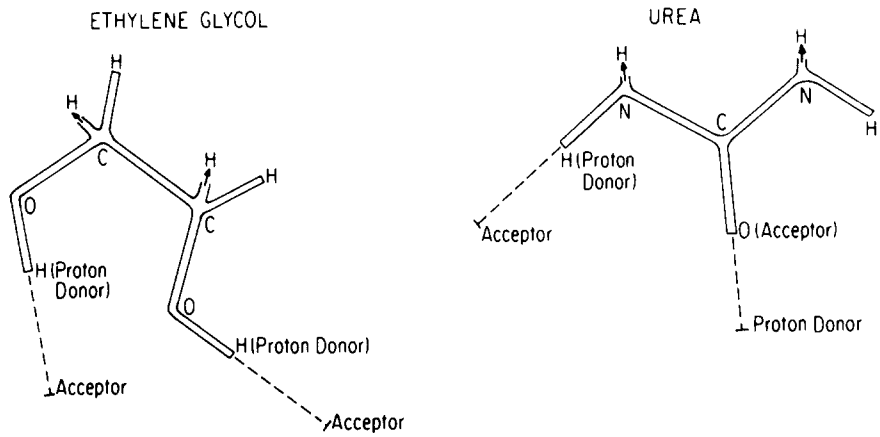


Fig. 9. Planar projections of Dreiding stick models showing selected H-bonds of urea and ethylene glycol.

equivalent pore of $\approx 6.5$ Å radius with hydrogen bond exchange regions at the entrance and exit, where the necessary exchange of the solute water of hydration with channel hydrogen bonds takes place [22,24]. This construct provides two types of loci in which the principal mechanisms of transport modulation take place. We denote the hydrogen bond exchange areas at the entrance and exist of the pore as 'H-bond-specific' regions, whose interactions depend upon the specific molecular configuration of the solute and are characterized by the dissociation constant, $K_{D,i}$. We denote the region between them, through which passage is controlled primarily by steric hindrance, as 'sieve-specific' regions. This construct has the advantage of providing a clear conceptual framework, though in the real membrane, the discrimination between the regions will not necessarily be sharp. Though we believe that the real red cell pore plays a role in the transport of charged ions, those properties are not at issue here and we will limit our considerations to the idealized pore in Fig. 8, whose functions are limited to the passage of nonelectrolytes and water.

We have used Dreiding stick Stereomodels (Brinkman Instruments, Inc., Westbury NY) to show the configuration of some of the principal H-bonding sites of urea and ethylene glycol. Fig. 9 shows planar projections of each molecule, in which selected donor (or acceptor) atoms in the solute are connected to the acceptor (or donor) in the H-bonding site by a dotted linear extension representing the H-bond. The rigidity of the amide bonds in urea places a firm constraint on the position of both the carbonyl O acceptor and the nitrogen H donor. The ethylene glycol molecule H-bonds have a great deal of rotational freedom, since each donor H can rotate about its O and the C-C bond also permits free rotation. The $K_m$ values for saturation of self-transport are very high ($K_{m,\ urea} = 218$ mM (Mayrand and Levitt [19]) and $K_{m,\ eth\ gly} = 220$ mM, this study), which means that there must be considerable latitude in the requirements for fit. Notwithstanding this latitude, Fig. 9 shows how difficult it would be for any single specific site to satisfy the very different constraints of amide and ethylene glycol binding, a difficulty that turns into an impossibility when we consider that the amide carbonyl O requires a proton *donor* and both the ethylene glycol OH's require *acceptors*. Nonetheless, the fact that both processes are saturable means that the binding requirements are real and that site/solute interactions are an essential component of membrane transport.

The experimental evidence suggests that the H-bonding sites for alcohol and amide transport are located adjacent to a non-polar region. There is abundant evidence that the oligomers of pore-forming membrane-spanning helices form a regular array in which the hydrophilic residues face the aqueous channel within the pore, and the lipophilic residues, on the other side of the helix, provide contact with membrane phospholipids. In such a pore constructed from amphipathic helices, the non-polar regions are within a very few angstroms of the aqueous channel, providing an environment which would favor binding of thiol analogues, as we have observed. In Fig. 8, we have shown a mosaic at the mouth of the pore, with amide-specific domains alternating with alcohol-specific domains. For clarity in Fig. 8, we have shown each domain as consisting of a relatively large cluster of like sites, but in practice the domains could be quite small with only one, or a very few specific binding sites per domain; in principle, though, the two types of domains would be in intimate contact.

Our construct conforms well to the structure of the nicotinic acetylcholine receptor, which has recently been reconstructed by Toyoshima and Unwin [28]. When the receptor is activated by chemical stimuli, cations diffuse through a water filled channel which forms the axis of a ring of five membrane-spanning helices. At the synaptic end, the channel consists of a tube, $\approx 60$ Å long, with a

uniform radius of about 12–13 Å. At the level of the outer phospholipid headgroups, the channel is constricted to a narrow pore, of radius probably less than 5 Å, which extends across the membrane to the inner phospholipid headgroups where the channel widens again to a broader tube, approximately 10 Å (or less) in radius which extends a further 15–20 Å into the cytoplasm. The model in Fig. 8 conforms very well to this structure, in which we could imagine incorporation of the H-bond-specific region as a component of the broad tubes at the inside and outside of the pore and representation of the sieve-specific region by the ≈ 5 Å channel through the membrane phospholipids.

*How does the low-affinity site work?*

The low-affinity water inhibition is presumably caused either by shrinkage of the sieve-specific passage or by interposition of an additional external barrier which impedes the flow of water at the H-bonding region at the entrance to and/or exit from the cell. This low-affinity gate is apparently controlled by sites similar to, but different from, those that control nonelectrolyte traffic. It is important to realize that the higher affinity nonelectrolyte transport sites are all filled before the low affinity inhibition takes place. The similarities between the higher and lower affinity sites include: the correlation of the amide $K_I$ values; and the observation that thiol compounds are more effective in promoting alcohol inhibition of water transport, just as they are in promoting amide inhibition of urea transport. The two sites behave as if they were two populations with similar characteristics, the primary nonelectrolyte transport sites which are located close enough to the channel wall to provide the higher affinity binding, and the secondary sites held further away from the channel wall by structural constraints which limit the closeness of solute approach, and hence decrease $K_I$.

It is possible to discriminate between dimensional changes which shrink the sieve-specific passage and effects on an external barrier by using the observations from the literature [29–31], that concentrations of ≈ 0.5 M urea have essentially no effect on the diffusional permeability of water, as Toon and Solomon [1] discussed. If results on bank blood, which Toon and Solomon used, are comparable with results on fresh blood, which the other investigators used, any process which shrinks the dimensions of the sieve-specific channel, should affect diffusional permeability as well as osmotic permeability. Although effects on diffusional permeability (which depend on the square of the channel radius) are smaller than those on osmotic permeability (which depend on the fourth power of the channel radius) the water transport inhibition which Toon and Solomon reported should have produced significant and detectable changes in the diffusional permeability. These considerations make it likely that the low-affinity gate is at the external approaches to the membrane rather than within the sieve-specific channel *.

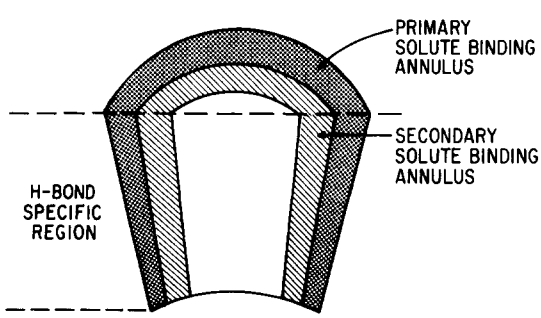


Fig. 10. Schematic cross-section of H-bonding region showing relative position of primary and secondary solute annuli.

The model which we propose to accomodate both high- and low-affinity sites is based on the observations of Longsworth [32] on the behavior of hydrogen bonding solutes, such as *N*-ethylacetamide and ethanol, in the non-polar solvent, $CCl_4$. *N*-Ethylacetamide, Longsworth found, associates into a nonionic micelle in $CCl_4$ of more than 100 monomeric units at a concentration of 0.2 molal; tetramers, at the least, are present at concentrations as low as 0.12 molal. Ethanol H-bonds significantly at 0.1 molal and a cyclic tetramer has been proposed as a stable structure in non-polar solvents. In view of the evidence suggesting that the urea binding site is close to non-polar helix residues and perhaps also

* There is a fundamental physical difference between the processes of diffusion and osmotic flow. Diffusion takes place molecule by molecule and there is no coupling between molecules diffusing in a dilute solution. In osmotic flow molecules travel in packets, which can transfer momentum to neighboring packets. This difference is best illustrated by passage through a capillary, in which diffusion (Fick's law) is proportional to the square of the radius (that is, the area), while osmotic flow (Poiseuille's law) is proportional to the fourth power of the radius. The fourth-power dependence arises because each annulus traversing the capillary in osmotic flow can transfer momentum to the adjacent annuli. If an obstruction is placed in a capillary, it will decrease the radius and impede both diffusion and osmotic flow, which are coupled within the capillary in the sense that one cannot be modified without affecting the other.

This is not the case at the entrance and exit to the capillary where obstructions can affect the streamlines of osmotic flow with minimal effects on diffusion. This can be visualized by comparing the properties of two imaginary septa placed near the entrance to a cylindrical channel. Let one septum be pierced by a single large hole whose area is such that diffusion is reduced by 50%. Let the second septum be pierced by a large number of small holes whose total area is the same as that of the single aperture in the first septum. Then, neglecting second order effects, the two diffusional barriers will offer equal resistance to diffusion. Yet because of the fourth power dependence of osmotic flow on radius, the second barrier will impede osmotic flow very much more effectively than the first. Thus obstructions to the streamlines of osmotic flow at the entrance to an aqueous channel can have large effects on osmotic flow with little or no hindrance to diffusion.

to membrane lipids, it is likely that the urea and ethylene glycol binding sites in the red cell are in a region appreciably less polar than water, a region in which dimeric association of urea and ethylene glycol would be promoted. The very large fluorescence enhancement [33] observed when the stilbene anion exchange inhibitor, DBDS (4,4′-dibenzamidostilbene-2,2′-disulfonate) binds to its specific site on band 3 is a consequence of the much lower polarity of the DBDS binding site than that of aqueous solution.

Our model of diffusion through the red cell pore builds on this concept by proposing that the high affinity H-bonding sites for the alcohols and amides form a primary annulus bound to the pore helices as shown in Fig. 10. When the primary annulus sites are filled, further amide (or alcohol) molecules, now present at concentrations of the order of 0.2 M, form dimers or higher multimers to make a secondary binding annulus, inside the primary ring, as shown in Fig. 10. The hydrated radius of urea [8] is 5.6 Å and the non-hydrated radius is 2.6 Å, which would provide significant steric barriers to passage, if the aqueous channel in the red cell is similar to the nicotinic acetylcholine receptor, whose entrance on the synaptic side is formed by a 12–13 Å radius tube. Occupation of sites within the secondary binding annulus would occlude the entrance to the pore, thus providing the mechanism for the low affinity inhibition of water flux. Although it is not possible to predict the $K_D$ values of binding to these complex sites, it seems likely that the combined $K_D$ would reflect, at least in some degree, the $K_D$ of binding to the primary annulus. Thus the annular concept provides a mean of rationalizing the correlation observed by Toon and Solomon [1].

*Experimental tests of pore model*

Our model of the red cell presupposes that the ethylene glycol and urea H-bonding sites are separate, though adjacent. We reasoned that it might be possible to saturate the urea/amide family of sites with a urea transport inhibitor and thus deform the protein and produce an allosteric effect on the ethylene glycol family of sites. We chose the aromatic urea transport inhibitor, 1-(3,4-dichlorophenyl)-2-thiourea (DCPTU) because Mayrand and Levitt [19] had reported that it inhibited urea transport with $K_I = 10$ μM, though in one experiment in our hands the $K_I$ was 90 μM. We chose an aromatic urea derivative to maximize the effect on the urea H-bonding sites at 50 μM, an upper limit set by solubility considerations since the alcohol in which it was necessary to dissolve DCPTU has permeability effects of its own. The use of an aromatic transport inhibitor avoided the osmotic pressure perturbations that would have been presented by inhibitors [1] such as propionamide ($K_I = 270$ mM) or 1,3-dimethylurea ($K_I = 20$ mM). We found that 50 μM DCPTU inhibited $\omega_{urea}$ by only $70 \pm 16\%$ (S.E., 5 expts.). In these same experiments, 50 μM DCPTU stimulated $\omega_{eth\ gly}$ by $19 \pm 13\%$, which is significant at $P < 0.05$ ($t$ test). It is

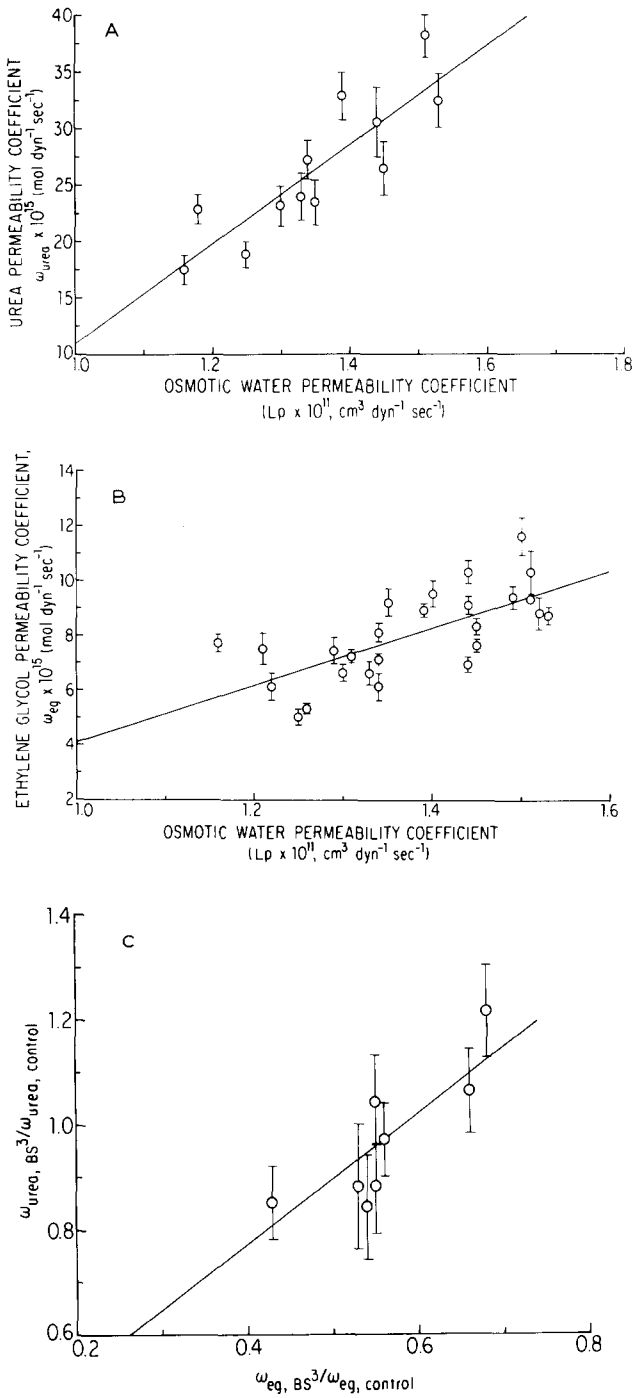


Fig. 11. (A) Dependence of urea permeability coefficient, $\omega_{urea}$, on hydraulic conductivity, $L_p$. Data from twelve experiments in $BS^3$ series. Least-squares fit with intercept $= -(33 \pm 11) \cdot 10^{-15}$ (mol·dyn$^{-1}$·s$^{-1}$) and slope $= (44 \pm 8) \cdot 10^{-4}$ (mol·cm$^{-3}$). (B) Dependence of ethylene glycol permeability coefficient, $\omega_{eth\ gly}$ on $L_p$. Data from 26 paired experiments as described in the text. Least-squares fit with intercept $= -(6 \pm 3) \cdot 10^{-15}$ (mol·dyn$^{-1}$·s$^{-1}$) and slope $= (10 \pm 2) \cdot 10^{-4}$ (mol·cm$^{-3}$). (C) Dependence of the urea ratio ($\omega_{urea,\ BS^3}/\omega_{urea,\ control}$) on the ratio ($\omega_{eth\ gly,\ BS^3}/\omega_{eth\ gly,\ control}$). Least-squares fit with intercept $= 0.3 \pm 0.2$ and slope $= 1.2 \pm 0.3$.

reasonable to ascribe the DCPTU inhibition of urea transport to simple competitive inhibition arising from DCPTU occupation of the urea sites in the H-bond-specific region. The observation that this inhibition is accompanied by *stimulation* of ethylene glycol fluxes suggests that binding of DCPTU leads to some conformational changes in the H-bond-specific region for ethylene glycol binding. The observation that lipophilic inhibitors of the urea family also can affect the permeability of ethylene glycol is consistent with the view that the H-bonding sites for the two families are in close apposition to one another.

We have also used chemical reagents which modify extracellular lysine and arginine residues in band 3 to provide further information about the aqueous channel. Bjerrum et al. [4] found that the arginine reagent, phenylglyoxal, binds to the 35 kDa segment of band 3 where it inhibits anion exchange at alkaline pH values. Under these conditions phenylglyoxal remains extracellular. Bjerrum et al. [4] have studied the distribution of labelled phenylglyoxal and report that there is little binding to the spectrin region, 54% is bound to band 3 and there is a smaller amount of additional binding in bands 5 and 6 and a little in band 7. Thus, phenylglyoxal is not solely a band 3 reagent, though binding of stilbene inhibitors interferes with that of phenylglyoxal.

Reaction with phenylglyoxal clearly stimulates water transport increasing $L_p$ by $10 \pm 2\%$ in eight experiments (standard error, $P < 0.01$, $t$ test). There was a concomitant rise in the ratio $\omega_{urea,\ phengly}/\omega_{urea,\ control}$ by $18 \pm 6\%$ in these experiments and in seven of them, the ratio $\omega_{ethgly,phengly}/\omega_{eth\ gly,\ control}$ was increased by $13 \pm 5\%$. Although there are large errors in the effects on urea and ethylene glycol fluxes, both of the increases are significant at $P < 0.05$ ($t$ test). These results suggest that phenylglyoxal modulates a channel common to water and the two nonelectrolytes.

We also carried out an extended series of experiments with $BS^3$, an impermeant reagent which Staros [34] showed to be a highly efficient cross-linker at physiological pH whose only cross-linked product is band 3. Jennings et al. [3] suggested that $BS^3$, which irreversibly inhibits $H_2$-DIDS binding, irreversibly modifies lysines *a* and *b* (in the notation of Passow [35]) and inhibits anion flux by more than 90%, when assayed above pH 8. Jennings et al. [3] argue that the effect is not due to steric blocking of access to the path, because the inhibitory effects can be overriden when the external pH is lowered. Salhany and Sloan [36,37] found that pretreatment of red cells with pyridoxal 5′-phosphate causes $BS^3$ treatment to cross-link band 3 into tetramers rather than dimers; furthermore, $BS^3$ also forms tetramers when the cells are pretreated with 0.5 mM DNDS (4,4′-dinitrostilbene-2,2′-disulfonate) and in this case, the effect is reversible. Both Staros and Salhany and Sloan used gels to show that oligomers had been formed, which provides convincing evidence that only band 3 is cross-linked, but does not preclude the reaction of $BS^3$ with extracellular lysine groups on other proteins that do not lead to oligomer formation.

We carried out twelve experiments with red cells, pretreated with $BS^3$ following the protocol of Jennings et al. [3], in which $L_p$ and $\omega_{urea}$ were measured. In the final eight experiments in this series, we also measured $\omega_{eth\ gly}$. The most striking observation was that $BS^3$ decreased the ratio $(\omega_{eth\ gly,\ BS^3}/\omega_{eth\ gly,\ control})$ to $0.53 \pm 0.01$, which shows that $BS^3$ reacts with the protein responsible for ethylene glycol permeation and strongly suggests that band 3 is the responsible protein. Although, on the average, $BS^3$ did not affect $L_p$, the mean ratio $(L_{p,\ BS^3}/L_{p,\ control})$ being $0.95 \pm 0.1$, the large value of the standard error of the mean shows that there is considerable excursion on either side of the mean. There was also no apparent effect of $BS^3$ on $\omega_{urea}$ since the ratio $(\omega_{urea,\ BS^3}/\omega_{urea,\ control})$ is $1.04 \pm 0.16$, but again there is a large excursion. These large excursions, not only in the $BS^3$ ratios, but also in the control values of $L_p$ and $\omega_{urea}$, led us to determine whether meaningful correlations lay hidden among the means. When we plotted $\omega_{urea}$ as a function of $L_p$, we found the clear correlation shown in Fig. 11A. The correlation coefficient, $r$, in these 12 experiments is 0.9 and the correlation is significant at $P < 0.01$ ($t$ test). This correlation means that as water passes through the channels with greater or less ease, so does urea. In the simplest terms, when the hole gets bigger, the flow increases. Although this is not a proof, it is a most persuasive argument and alternative explanations are more labored and require extensive constructs.

Since the aqueous channel hypothesis supposes that ethylene glycol crosses the membrane in the water channel, we expected to find a similar correlation between $\omega_{eth\ gly}$ and $L_p$. There are only eight experiments in which this comparison can be made in the $BS^3$ series, but there are 18 other suitable pairs in the other experiments on $\omega_{eth\ gly}$ and $\sigma_{eth\ gly}$. Fig. 11B shows that $\omega_{eth\ gly}$ is also correlated with $L_p$, with a correlation coefficient of 0.69 which is significant at $P < 0.01$ ($t$ test). This correlation is entirely consistent with flow of ethylene glycol and water through the same channel and, as in the case of urea, any other explanation requires additional ad hoc assumptions.

It seems logical to assign the individual differences in $L_p$ from one blood to another to small changes in the pore diameter, due to small differences in the close packing between the helices that make up the pore. This line of reasoning would assign the correlations in Figs. 11 A and B to interactions in the steric region of the pore. Since ethylene glycol and urea are similar in size, it is logical to inquire whether the hindrance to passage offered by the sieve-specific region is similar for these two chemically dissimilar molecules. To make this com-

parison, we first determined the average $L_p$ of $1.38 \cdot 10^{-11}$ cm$^3 \cdot$ dyn$^{-1} \cdot$ s$^{-1}$ for the 26 experiments in Fig. 11B and then computed the normalized $\omega_{\text{eth gly},0} = 7.6 \cdot 10^{-15}$ mol $\cdot$ dyn$^{-1} \cdot$ s$^{-1}$ and $\omega_{\text{urea},0} = 28 \cdot 10^{-15}$ mol $\cdot$ dyn$^{-1} \cdot$ s$^{-1}$ at this $L_p$, using the coefficients given in the legends to Figs. 11 A and B. For larger pores, $L_p$ becomes larger as do $\omega_{\text{eth gly}}$ and $\omega_{\text{urea}}$; the slope of the line $(d\omega/d(L_p)$ provides a measure of the coupling between solute and water fluxes as a function, as it were, of pore radius. In order to compare these slopes, it is necessary to normalize them, which we can do by defining a normalized coupling coefficient for the relative hindrance to passage of solute and water through the sieve-specific region, $\gamma = d(\omega/\omega_0)/d(L_p)$. This computation leads to $\gamma_{\text{eth gly}} = 1.6 \cdot 10^{11}$ dyn $\cdot$ s $\cdot$ cm$^{-3}$, which is exactly the same as $\gamma_{\text{urea}} = 1.6 \cdot 10^{11}$ dyn $\cdot$ s $\cdot$ cm$^{-3}$. The identity of these $\gamma$ values for two such chemically dissimilar but similarly sized molecules * is just what might be expected for passage of solute and solvent together through the sieve-specific region of the pore.

Fig. 11C shows another correlation hidden among the means, the relation between $\omega_{\text{eth gly}}$ and $\omega_{\text{urea}}$ in eight experiments. The ratio $(\omega_{\text{urea, BS}^3}/\omega_{\text{urea, control}})$ is linearly dependent upon the ratio $(\omega_{\text{eth gly, BS}^3}/\omega_{\text{eth gly, control}})$ with a correlation coefficient of 0.84 which is significant at $P < 0.01$ ($t$ test). These data show that the passage of urea across the membrane is correlated with that of ethylene glycol. Thus, when BS$^3$ perturbs the channel sufficiently to decrease ethylene glycol transport by 47%, the perturbation in the channel is accompanied by a proportional effect on urea permeability. This relationship is entirely consistent with expectations based on a shared pathway. In particular, it is difficult to imagine a simple alternative mechanism which would account for the proportionality between these effects of BS$^3$.

When we first embarked on the systematic investigation of the three phenomenological coefficients that describe the permeability of the short-chain alcohols, we did not realise that these measurements would provide the key to so many revealing aspects of the permeability process. They have shown us that:

(1) The solute/membrane friction, $f_{sm}$, decreases systematically with membrane permeability, entirely consistent with flow through an aqueous pore, as shown in Fig. 3.

(2) The experiments with DCPTU show that inhibition of urea permeability by a lipophilic urea derivative is accompanied by stimulation of ethylene glycol flux.

(3) Treatment with phenylglyoxal leads to a stimulation of water flux which is accompanied by stimulation of both urea and ethylene glycol fluxes.

(4) Treatment with BS$^3$ leads to effects on both ethylene glycol and urea permeability, and these effects are correlated, as shown in Fig. 11C.

(5) In the 12 experiments in the BS$^3$ series, increases in water permeability are correlated with increases in urea permeability, as shown in Fig. 11A.

(6) In 26 experiments, increases in water permeability are correlated with increases in ethylene glycol permeability, as shown in Fig. 11B.

(7) The fractional increase in urea permeability, as water permeability increases, is the same as the fractional increase of ethylene glycol permeability.

All of these seven observations are consistent with the proposition that water, urea and ethylene glycol cross the membrane in the same aqueous pore, but no single one is proof. However, the cumulative weight of the evidence is impressive as can be seen from the following calculation. Let us assume that in each of these seven cases, the probability that the observation is correlated with the existence of an aqueous channel is two out of three; that is the probability that the correlation is due to chance is one in three. The probability that all seven correlations are due to chance is $\ll 0.001$ $(5 \cdot 10^{-5})$. Indeed if the chance were one in two, the probability would still be $< 0.01$ [0.0078]. When these considerations are taken together with the observation that in 29 experiments, $\sigma_i$ for the alcohols is significantly less than unity, it is very difficult to resist the conclusion that the hydrophilic alcohols and urea cross the red cell membrane in the same aqueous channel.

* Orthogonal molecular dimensions measured on CPK models are: urea, 5.2×5.8×3.2 Å; ethylene glycol, 5.8×4.8×4.2 Å.

## References


1 Toon, M.R. and Solomon, A.K. (1988) Biochim. Biophys. Acta 940, 266–274.
2 Terwilliger, T.C. and Solomon, A.K. (1981) J. Gen. Physiol. 77, 549–570.
3 Jennings, M.L., Monaghan, R., Douglas, S.M. and Nicknish, J.S. (1985) J. Gen. Physiol. 86, 653–669.
4 Bjerrum, P.J., Wieth, J.O. and Borders, C.L. Jr. (1983) J. Gen. Physiol. 81, 453–484.
5 Goldstein, D.A. and Solomon, A.K. (1960) J. Gen. Physiol. 44, 1–17.
6 Chasan, B. and Solomon, A.K. (1985) Biochim. Biophys. Acta 821, 56–62.
7 Levin, S.W., Levin, R.L. and Solomon, A.K. (1980) J. Biochem. Biophys. Methods 3, 255–272.
8 Toon, M.R. and Solomon, A.K. (1987) Biochim. Biophys. Acta 898, 275–282.
9 Sha'afi, R.I., Rich, G.T., Mikulecky, D.C. and Solomon, A.K. (1970) J. Gen. Physiol. 55, 427–450.
10 Jay, A.W.L. (1975) Biophys. J. 15, 205–222.
11 Savitz, D., Sidel, V.W. and Solomon, A.K. (1964) J. Gen. Physiol. 48, 79–91.
12 Solomon, A.K., Toon, M.R. and Dix, J.A. (1986) J. Membr. Biol. 91, 259–273.
13 Solomon, A.K. (1989) in Methods of Enzymology, Vol. 173, (Fleischer, S. and Fleischer, B., eds.), pp. 192–222, Academic Press, New York.

14 Sha'afi, R.I., Gary-Bobo, C.M. and Solomon, A.K. (1971) J. Gen. Physiol. 58, 238–258.
15 Kedem, O. and Katchalsky, A. (1958) Biochim. Biophys. Acta 27, 229–246.
16 Dainty, J. (1963) Adv. Bot. Res. 1, 279–326.
17 Katchalsky, A. and Curran, P.F. (1965) Nonequilibrium Thermodynamics in Biophysics, Harvard University Press, Cambridge, MA.
18 Levitt, D.G. and Mlekoday, H.J. (1983) J. Gen. Physiol. 81, 239–253.
19 Mayrand, R.R. and Levitt, D.G. (1983) J. Gen. Physiol. 81, 221–237.
20 Rich, G.T., Sha'afi, R.I., Romualdez, A. and Solomon, A.K. (1968) J. Gen. Physiol. 52, 941–954.
21 Savitz, D. and Solomon, A.K. (1971) J. Gen. Physiol. 58, 259–266.
22 Solomon, A.K., Chasan, B., Dix, J.A., Lukacovic, M.F., Toon, M.R. and Verkman, A.S. (1983) Ann. NY. Acad. Sci. 414, 97–124.
23 Ginzburg, B.Z. and Katchalsky, A. (1963) J. Gen. Physiol. 47, 403–418.
24 Solomon, A.K. (1986) J. Membr. Biol. 94, 227–232.
25 Collander, R. (1954) Physiol. Plantarum 7, 420–445.
26 Wieth, J.O., Funder, J., Gunn, R.B. and Brahm, J. (1974) in Comparative Biochemistry and Physiology of Transport (Bolis, L., Bloch, K., Luria, S.E. and Lynen, F., eds.), pp. 317–337, North-Holland Publishing, Amsterdam.
27 Solomon, A.K. and Chasan, B. (1980) Fed. Proc. 39, 957a.
28 Toyoshima, C. and Unwin, N. (1988) Nature 336, 247–250.
29 Brahm, J. (1982) J. Gen. Physiol. 79, 791–819.
30 Chien, D.Y. and Macey, R.I. (1977) Biochim. Biophys. Acta 464, 45–52.
31 Fabry, M.E. and Eisenstadt, M. (1978) J. Membr. Biol. 42, 375–398.
32 Longsworth, L.G. (1966) J. Colloid Interface Sci. 22, 3–11.
33 Verkman, A.S., Dix, J.A. and Solomon, A.K. (1983) J. Gen. Physiol. 81, 421–449.
34 Staros, J.V. (1982) Biochemistry 21, 3950–3955.
35 Passow, H. (1986) Rev. Physiol. Biochem. Pharmacol. 103, 62–223.
36 Salhany, J.M. and Sloan, R.L. (1988) Biochem. Biophys. Res. Commun. 156, 1215–1222.
37 Salhany, J.M. and Sloan, R.L. (1989) Biochem. Biophys. Res. Commun. 159, 1337–1344.